HHS Public Access

Author manuscript

Ann Hum Genet. Author manuscript; available in PMC 2023 May 28.

Published in final edited form as:

Ann Hum Genet. 2021 March ; 85(2): 80–91. doi:10.1111/ahg.12411.

Identification and functional study of genetic polymorphisms in cyclic nucleotide phosphodiesterase 3A (*PDE3A*)

You Ran Kim[1], **MyeongJin Yi**[1,2], **Sun-Ah Cho**[1], **Woo-Young Kim**[1], **JungKi Min**[3], **Jae-Gook Shin**[1,4], **Su-Jun Lee**[1]

[1]Department of Pharmacology and Pharmacogenomics Research Center, Inje University College of Medicine, Inje University, Busan, South Korea

[2]Pharmacogenetics Section, Reproductive and Developmental Biology Laboratory, National Institute of Environmental Health Sciences, National Institutes of Health, Research Triangle Park, North Carolina, USA

[3]Genome Integrity and Structural Biology Laboratory, National Institute of Environmental Health Sciences, NIH, Research Triangle Park, North Carolina, USA

[4]Department of Clinical Pharmacology, Inje University Busan Paik Hospital, Inje University College of Medicine, Inje University, Busan 47392, South Korea

Abstract

Phosphodiesterase 3A (PDE3A) is an enzyme that plays an important role in the regulation of cyclic adenosine monophosphate (cAMP)–mediated intracellular signaling in cardiac myocytes and platelets. PDE3A hydrolyzes cAMP, which results in a decrease in intracellular cAMP levels and leads to platelet activation. Whole-exome sequencing of 50 DNA samples from a healthy Korean population revealed a total of 13 single nucleotide polymorphisms including five missense variants, D12N, Y497C, H504Q, C707R, and A980V. Recombinant proteins for the five variants of PDE3A (and wild-type protein) were expressed in a FreeStyle 293 expression system with site-directed mutagenesis. The expression of the recombinant PDE3 Aproteins was confirmed with Western blotting. Catalytic activity of the PDE3A missense variants and wild-type enzyme was measured with a PDE-based assay. Effects of the missense variants on the inhibition of PDE3A activity by cilostazol were also investigated. All variant proteins showed reduced activity (33–53%; $p < .0001$) compared to the wild-type protein. In addition, PDE3A activity was inhibited by cilostazol in a dose-dependent manner and was further suppressed in the missense variants. Specifically, the PDE3A Y497C showed significantly reduced activity, consistent with the predictions of in silico analyses. The present study provides evidence that individuals carrying

Correspondence Su-Jun Lee, Department of Pharmacology and Pharmacogenomics Research Center, Inje University College of Medicine, Inje University, Bokji-ro 75, Busanjin-gu, Busan 47392, South Korea. 2sujun@inje.ac.kr.
You Ran Kim and MyeongJin Yi contributed equally to this work.

AUTHOR CONTRIBUTIONS

Study design: SJL and JGS; data collection and analysis: YRK, MJI, SAC, WYK, and JKM; interpretation and manuscript preparation: MJY, YRK, and SJL.

SUPPORTING INFORMATION

Additional supporting information may be found online in the Supporting Information section at the end of the article.

CONFLICT OF INTEREST

The authors report no potential conflicts of interest.

the PDE3A Y497C variant may have lower enzyme activity for cAMP hydrolysis, which could cause interindividual variation in cAMP-mediated physiological functions.

Keywords

adenylyl cyclase; cilostazol; genetic polymorphisms; phosphodiesterase 3A (PDE3A); single nucleotide polymorphism

1 | INTRODUCTION

Cyclic-nucleotide phosphodiesterases (PDEs) have an important role in intracellular signaling mediated by cyclic adenosine monophosphate (cAMP) and cyclic guanosine monophosphate (cGMP) (Ahmad et al., 2015; Rybalkin, Yan, Bornfeldt, & Beavo, 2003). The PDE enzyme super-family can be grouped into 11 different families, from *PDE1* to *PDE11*, in humans (Azevedo et al., 2014). Isoforms of the PDE3 family, which hydrolyze cAMP and cGMP, are of particular importance in the context of cardiac and vascular smooth muscle (Francis, Busch, Corbin, & Sibley, 2010; Movsesian, Ahmad, & Hirsch, 2018). Human *PDE3* genes, also referred to as cGMP-inhibited PDEs, include *PDE3A* and *PDE3B* (Palmer & Maurice, 2000). PDE3A proteins exist in three isoforms that are derived from a single gene and the same transcript (Y. H. Choi et al., 2001). PDE3A1 expression sites are commonly found in cardiac myocytes (Ahmad et al., 2015; Wechsler et al., 2002) and platelets (Berger et al., 2020). PDE3A2 is the dominant isoform in vascular cells (Ercu et al., 2020; C. G. Lee, Kang, Yoon, Seo, & Park, 2020; Traylor et al., 2020) and PDE3A3 is a major form in placenta (Y. H. Choi et al., 2001). PDE3B is expressed in adipocytes (Heemskerk et al., 2014), hepatocytes, pancreatic beta cells (Degerman et al., 2011), T lymphocytes (Kress et al., 2010), and cardiomyocytes (Chung et al., 2015). PDE3A is either membrane associated or cytosolic, depending on the variant and cell type, whereas PDE3B is predominantly localized in the membrane (Reinhardt et al., 1995).

Currently, two PDE3 selective inhibitors are used clinically: cilostazol and milrinone. Cilostazol is an antiplatelet agent with antithrombotic and vasodilatory effects. It has been approved to treat patients with intermittent claudication and to prevent short- and medium-term vessel closure as well as late restenosis after intracoronary stenting (H. I. Choi et al., 2018). Milrinone improves the hemodynamics of heart failure via vasodilatory effects triggered by increased cardiac intracellular cAMP levels (Teerlink, 2009), but it also has strong inotropic effects (Thorlacius et al., 2020). Milrinone has been used to treat perioperative severe heart failure and to counteract the marked deterioration caused by congestive heart failure (Zewail et al., 2003).

Recent studies have reported an association between genetic polymorphisms in *PDE3A* and risk for cardiovascular disease (Ercu et al., 2020; Traylor et al., 2020). PDE3A is involved in regulating cellular levels of cAMP, an important signaling molecule for the platelet function. This has sparked further study into the role of *PDE3A* genetic variants in platelet activation and cardiovascular disease (Kato et al., 2015; Traylor et al., 2020). Because elevated levels of cAMP inhibit pathways of platelet activation, elucidating the effects of PDE3A activity on cAMP levels is crucial for understanding the pathophysiological response to

the antiplatelet therapy (Ahmad et al., 2015). Changes in PDE3A expression or function due to genetic mutations affect cAMP hydrolysis and interfere with antiplatelet therapies, such as cilostazol (Rondina & Weyrich, 2012). In the present study, we identified genetic polymorphisms in the *PDE3A* gene and characterized their functional differences compared to wild-type PDE3A1 using a recombinant enzyme system. Our results may provide useful information for increasing the therapeutic efficacy of antiplatelet therapies while shedding light on other important related genes.

2 | MATERIALS AND METHODS

2.1 | Chemicals

Sodium dodecyl sulfate (SDS), bovine serum albumin (BSA), dimethyl sulfoxide (DMSO), ethylenediaminetetraacetic acid (EDTA), nonyl phenoxypolyethoxylethanol (NP-40), hydrochloric acid (HCl), tris-base, sodium chloride (NaCl), potassium chloride (KCl), sodium phosphate diabasic (Na_2HPO_4), potassium phosphate monobasic (KH_2PO_4), and ammonium persulfate, *N*,*N*,*N*′,*N*′-tetramethylethylenediamine were all purchased from Sigma-Aldrich (St. Louis, MO, USA). Skimmed milk was manufactured by BD Difco Laboratories, a subsidiary of Becton, Dickinson and Company (Sparks, MD, USA). Boric acid, lysogeny broth (LB), and LB agar mixture were obtained from USB (Cleveland, OH, USA). Bradford protein assay reagents and 30% bisacrylamide solution were purchased from Bio-Rad Laboratories (Hercules, CA, USA). Methyl and ethyl alcohols were produced by Honeywell Burdick & Jackson (Muskegon, MI, USA). Ex-Taq polymerase, 10× Ex-Taq buffer, and dNTP mixture were obtained from Takara Bio (Otsu, Japan). Western Blotting Luminol Reagent, primary antibody for glyceraldehyde-3-phosphate dehydrogenase (GAPDH), PDE3A, and secondary antibodies (goat and mouse) were purchased from Santa Cruz Biotech (Dallas, TX, USA). Serum-free FreeStyle™ medium was produced by Gibco Invitrogen (Carlsbad, CA, USA). All chemicals used in the experiments were analytical grade.

2.2 | Subjects and DNA samples

Genomic DNA samples ($n = 50$: 33 males and 17 females) were obtained from the DNA Repository Bank of the Pharmacogenomics Research Center (Inje University College of Medicine, Busan, South Korea) as reported previously (S. J. Lee, Kim, Choi, Lee, & Shin, 2010). A consent was obtained from all healthy subjects with no drug administration, and the research protocol was approved by the institutional review board of Inje University Busan Paik Hospital, Busan, South Korea.

2.3 | Identification of genetic variants

We isolated each genomic DNA sample from peripheral blood using the QIAamp DNA Blood Kit (Qiagen, Hilden, Germany). Coding regions were amplified with SureSelect (Agilent Technologies, Santa Clara, CA, USA), and paired-end sequencing of base pairs was performed on an Illumina HiSeq2500 Platform (Illumina Cambridge, Cambridge, UK) as described previously (Yi et al., 2017). We aligned sequence data using a BWA-MEM algorithm and analyzed it using SureCall 2.1 (Agilent Technologies). Exome data were analyzed with an average coverage depth of 4× to identify rare variants. To confirm the

rare variants identified by *PDE3A* exome sequencing, we amplified *PDE3A* exons using the polymerase chain reaction (PCR). We purified PCR products using a PCR purification kit (NucleoGen, Ansan, South Korea) and directly sequenced purified samples using an ABI Prism 3700Xi Genetic Analyzer (Applied Biosystems, Waltham, MA, USA) to confirm the mutation. All primers used in *PDE3A* exome sequencing are described in Supplement Table 1.

2.4 | Construction of PDE3A variants using site-directed mutagenesis

We constructed the *PDE3A* mutants D12N, Y497C, H504Q, C707R, and A980V using a QuikChange site-directed mutagenesis kit (Stratagene, La Jolla, CA, USA) with specifically designed primers (Supplement Table 2). Briefly, the reaction included 50 ng pcDNADEST40 containing wild-type *PDE3A* cDNA, dNTPs, and *Pfu* DNA polymerase in accordance with the manufacturer's instructions (Stratagene) (Suzuki et al., 2005). PCR was performed as follows: 16 cycles of 95°C for 30 s, 55°C for 1 min, and 68°C for 10 min. We linearized the parental template plasmid by treating it with endonuclease *DpnI* (10 units/mL; Boehringer Mannheim, Ingelheim am Rhein, Germany) for 3 hr. Subsequently, the doublenicked recombinant pcDNA-DEST40 was used to transform competent XL1-Blue cells (Stratagene). All recombinant plasmids were analyzed by direct DNA sequencing to confirm mutations.

2.5 | Expression of PDE3A in FreeStyle 293-F cells

PDE3A wild-type and variant proteins were produced in FreeStyle 293-F cells (Invitrogen). Briefly, 293-F cells were transfected with the recombinant pcDNA-DEST40 vectors using 293 fectin (Invitrogen) and then grown in serum-free FreeStyle 293 expression medium for 36 hr. Transfected 293-F cells were harvested and resuspended in the lysis buffer (50 mM KCl, 1 mM dithiothreitol [DTT], 50 mM *N*-2-hydroxyethylpiperazine-N′−2-ethanesulfonic acid [HEPES] KOH [pH 7.2], 10 mM ethylene glycol-bis(*β*-aminoethyl ether)-*N*,*N*,*N*′,*N*′-tetraacetic acid [EGTA], 1.92 mM $MgCl_2$, 10% glycerol, and protease inhibitors), and the membrane fraction was isolated as described previously (Suzuki et al., 2005).

2.6 | Extraction of RNA and reverse transcriptase-polymerase chain reaction

Total RNA samples from FreeStyle 293-F cells expressing recombinant proteins were extracted with TRIzol reagent (Invitrogen). Each RNA sample was quantified using a NanoDrop 2000 spectrophotometer (Thermo Fisher Scientific, Waltham, MA, USA), measuring at absorbances of 260 and 280 nm. We synthesized cDNA samples by adding 1 *μ*g total RNA to a reaction mixture of 100 pmol/L oligo (dT) 18, 2.5 mM dNTP, and RNAse-free water to a total volume of 27 *μ*L. After heating, 0.1 M DTT, 5× first strand buffer, and 200 units M-MLV reverse transcriptase were added. The samples were incubated at 42°C for 1 hr. The reaction was terminated by adjusting the temperature to 72°C for 5 min. The synthesized cDNA samples were amplified by PCR (25 cycles) in a 50-*μ*L reaction volume containing 10 mM dNTP, 25 mM $MgCl_2$, 10 pmol/L forward and reverse primers, and 1 unit Ex-Taq DNA polymerase (Takara Bio). We used Primer-BLAST (https://www.ncbi.nlm.nih.gov/tools/primer-blast/) to design each of the primers to target the *PDE3A* gene. The forward primer was 5′-AAATGATGGTTGGGTTCTGG-3′, and the reverse primer was 5′-CTGAATATAGGGCACCCTCAG-3′. The reaction was performed as

follows: 94°C for 3 min to allow initial denaturation; 25 cycles of denaturation at 94°C for 20 s, annealing at 58°C for 30 s, and elongation at 72°C for 1 min; and a final cycle of elongation at 72°C for 5 min. The amplified DNA was separated on a 1% (w/v) agarose gel, and the gel was stained with ethidium bromide for visualization.

2.7 | Protein extraction and Western blotting analyses

After cells were transfected with recombinant plasmids or an empty vector for 36 hr, total cell lysates were prepared for further analyses. Briefly, FreeStyle 293-F cells, diluted to 1.5 × 10^5 cells/mL, were transfected and incubated for 36 hr. Harvested cells were resuspended in cell lysis buffer (50 mM KCl, 1 mM DTT, 50 mM HEPES KOH [pH 7.2], 10 mM EGTA, 1.92 mM $MgCl_2$, 20% glycerol, and protease inhibitors), and cells were disrupted by sonication for 10 s with a 30-s interval on ice, repeated five times. Cell debris was removed by centrifugation at 15,000 *g* for 30 min. The supernatant was stored at −80°C and used for Western blotting or functional activity assays. Each protein sample (30 μg/lane) was separated by sodium dodecyl sulfate polyacrylamide gel electrophoresis (SDS-PAGE) and transferred to activated polyvinylidene difluoride (PVDF) membranes (GE Healthcare, Chicago, IL, USA). The membranes were blocked with 5% skimmed milk in Tris-buffered saline and Tween 20 buffer (TBS-T; 10 mM Tris, 150 mM NaCl [pH 7.5], and 0.1% Tween 20) for 1 hr at room temperature (RT), and then samples were incubated with primary antibodies for *PDE3A* (diluted 1:500) overnight at 4°C. The membranes were washed four times for 5 min in TBS-T buffer and then incubated for 1 hr with horseradish peroxidase-conjugated secondary antibodies. The membranes were washed four times for 10 min with TBS-T buffer. Protein bands were visualized with an enhanced chemiluminescence (ECL) substrate (Amersham-Pharmacia Biotech, Little Chalfont, UK) on Kodak Biomax MR film (Eastman Kodak, Rochester, NY, USA). Immunoblot analysis of GAPDH was used as a loading control. The data were quantified with Image J version 1.43 (National Institutes of Health, Bethesda, MD, USA).

2.8 | In silico analyses of protein stability

PolyPhen 2.0, Sorting Intolerant from Tolerant (SIFT), and I-Mutant 3.0 were used to predict functional changes in *PDE3A* associated with single nucleotide polymorphisms (SNPs) in protein coding regions. PolyPhen 2.0 focuses on a combination of protein sequence and structure using a Bayesian classifier to identify amino acid substitutions to model the impact of a mutation on the protein structure. The output terms of “probably damaging” and “possibly damaging” were classified as functionally significant (≥0.51), and the “benign level” was classified as functionally tolerated (≤0.51) (Adzhubei et al., 2010). SIFT prediction focuses on the sequence homology and physicochemical properties of amino acids that are disrupted by substitution mutations. A SIFT score ≤0.05 indicates that the amino acid substitution is functionally intolerant or deleterious, whereas a score ≥0.05 is classified as tolerant (Kumar, Henikoff, & Ng, 2009). I-Mutant 3.0 is a support vector machine–based tool. We used the sequence-based version of I-Mutant 3.0, which has three classes of prediction: a neutral mutation (−0.5 ≤ DDG ≤ 0.5 kcal/moL), a large decrease (<−0.5 kcal/moL), or a large increase (>0.5 kcal/moL). The free energy change (ΔΔG) predicted by I-Mutant 3.0 is based on the difference between the unfolding Gibbs

free energy change in the mutant and native proteins (kcal/moL) (Capriotti, Fariselli, Rossi, & Casadio, 2008).

2.9 | Measurement of PDE activity

We measured PDE3A activity in a 96-well plate using a PDE-Glo Phosphodiesterase Assay (Promega, Madison, WI, USA). The PDE3A activity of each variant was analyzed according to the manufacturer's instructions. Briefly, a reaction mixture of 0.1 mL containing 30 μg prepared protein, 2 μM cAMP, and 20 μM cGMP in the absence or presence of cilostazol (0.1−1 μM) was incubated for 20 min at RT. Next 50 μL kinase-Glo reagent was added and incubated for 10 min at RT. After terminating the reaction with termination buffer, we added PDE-Glo detection solution and kinase-Glo reagent and immediately measured the luminescence of each sample using a Victor Multiplate Reader (Perkin Elmer, Waltham, MA, USA) (Ahmad et al., 2015).

2.10 | Prediction of phosphorylation

NetPhos3.1 (http://www.cbs.dtu.dk/services/NetPhos/, DTU Health Tech, Denmark) and PhosphoNet (http://www.phosphonet.ca/kinasepredictor.aspx?uni=P31751&ps=S130), Kinexus Bioinformatics Corp., Canada) were used to predict phosphorylated sites and identify protein kinases. Briefly, NetPhos3.1 predicts phosphorylation sites in eukaryotic proteins using a specific sequence in FASTA format. After submitting PDE3A sequence (NM_000921.5), each candidate position of residue was analyzed and output score was showed in the range from 0.000 to 1.000 depending on the relevance. PhosphoNet predicted the phosphorylated sites based on the number of experimentally confirmed sites and the percentage of phosphorylated sites relative to the total number in randomized studies after submitting international protein ID. Possible scores were based on analysis of the phosphosite independent of any other nearby phosphosites that might be recognized by the kinase shown with the maximum predicted score 1000.

2.11 | Statistical analyses

All datasets were analyzed by the Shapiro–Wilk test for normality evaluation, and they meet the assumption of normality. Data were analyzed by one-way analysis of variance (ANOVA), and Dunnett's tests for post hoc multiple comparisons. All of analyses and graphical visualizations were performed through Prism 8.2.1 (GraphPad Software, San Diego, CA, USA). All data are described as means ± SD of each independent value. p-Values < .05 were considered as statistically significant.

3 | RESULTS

Thirteen variants of *PDE3A* were identified (Table 1). Seven SNPs were detected in exons, and six SNPs were located in introns. Five SNPs resulted in amino acid substitutions: g.20369318G > A coding for D12N, 20621361A > G coding for Y497C, g.20621383T > A coding for H504Q, g.20637217T > C coding for C707R, and g.20653960C > T coding for A980V (Figure 1). Among them, g.20653960C > T was identified as a novel variant with a heterozygous mutation. Chi-square tests were used to analyze the discovered variants, and all of the allele frequencies were in the Hardy–Weinberg equilibrium (p > .05). To

analyze the genetic structure of the *PDE3A* locus in a Korean population, we performed a pairwise LD analysis using Haploview version 4.1; the result was no LD block (data not shown). A strong LD ($D' = 1$) was not found in pairwise comparisons of SNPs. The possibility of phosphorylation reaction was analyzed by NetPhos3.1 and PhosphoNet. According to NetPhos3.1, Y497 in the sequence context of FTSSYAISA was predicted to be phosphorylated (prediction score: 0.882 out of 1 with unspecific kinase) among the missense variants. The PhosphoNet predicted a phosphorylation at Y497 in the sequence context of SRSFTSSYAISAANH. Among plenty of candidates, five of most related kinases were predicted as SRMS (Q9H3Y6; src-related kinase lacking C-terminal regulatory tyrosine and N-terminal myristylation sites), PTK2 (Q05397; protein tyrosine kinase 2), BTK (Q06187; Bruton tyrosine kinase), TYRO3 (Q06418; TYRO3 protein tyrosine kinase), and MET (P08581; MET proto-oncogene), and each prediction score was 319, 312, 311, 311, and 309, respectively.

The recombinant *PDE3A* cDNA samples coding for amino acid changes were prepared by site-directed mutagenesis. Because the PDE3A protein requires phosphorylation as a posttranslational modification to be in an active form, FreeStyle293-F cells derived from the human embryonic kidney were used for functional analyses. Expression of each mutant and wild-type protein was examined in immunoblot analyses, which revealed a single band of the expected size of 135 kDa (Figure 2a). Western blotting showed that the expression of PDE3A was lower in the D12N, Y497C, and A980V variant proteins from transfected FreeStyle 293-F cells than in the wild-type protein. Specifically, the PDE3A protein variant Y497C showed the lowest expression of all PDE3A variant proteins in three independent transfections. Low expression or decreased stability of the protein caused by a mutation can influence functional activity. To determine whether the lower PDE3A in the Y497C variant protein was caused by a lack of protein stability, we compared mRNA levels of PDE3A in the Y497C variant protein to PDE3A wild-type mRNA by the reverse transcriptase-polymerase chain reaction (RT-PCR). The results indicated similar levels of mRNA between the mutant and the wild-type protein (Figure 2b). We determined the catalytic activity of the variant proteins using a PDE-Glo PDE assay system (Figure 3). Proteins prepared from cells transfected with an empty vector exhibited no activity. All variant proteins showed decreased activity, accounting for about half of the wild-type PDE activity (33−53%; $p < .0001$). In experiments examining PDE3A protein levels, the PDE3A Y497C variant showed the most significantly reduced activity among the five missense variants compared to the wild-type PDE3A protein. Finally, measurements revealed that the PDE3A Y497C variant proteins showed the highest sensitivity to cilostazol, followed by PDE3A A980V, D12N, H504Q, and C707R (Figure 4). Cilostazol reduced the activity of all of the variant proteins in a dose-dependent manner.

4 | DISCUSSION

In the present study, we identified genetic variants of the *PDE3A* gene, including five missense SNPs, and determined their functional differences compared to the PDE3A wild-type protein by testing for heterologous expression and enzyme activity. Our results provide information on the distribution of *PDE3A* genetic polymorphisms. All of the genetic variants of *PDE3A* identified in the present study have been reported in the 1000 Genomes database,

except for one missense variant (g.20653960C > T, A980V). The frequencies of the *PDE3A* missense variants discovered—g.20369318G > A, g.20621361A > G, g.20621383T > A, g.20637217T > C, and g.20653960C > T—were 28%, 2%, 4%, 1%, and 1%, respectively. Among the five missense mutations, D12N showed the highest frequency, 50.61% in African ancestry populations, 30.91% in Europeans, and 25.50% in Koreans. Of the 13 mutants discovered, the D12N and the g.20650332G > A (rs10770682) showed high frequency in African ancestry populations. On the other hand, the intron 14 variant, g.20650615T > C (rs10743384), had the lowest frequency in populations of African ancestry compared to other populations. In this study, no distinctive between ancestry-group frequency differences were found except for these variants. Genetic polymorphisms in the critical domain of the PDE3A protein affect enzyme activity. All variant proteins showed reduced activity compared to the wild-type protein. It is important to note that our results indicate that the Y497C missense variant of *PDE3A* is significantly limited in activity compared to the wild-type protein according to measured PDE3A protein levels. Activity of PDE3A enzyme can be affected by protein stability and phosphorylation status. A mutant-specific alteration of the phosphorylation has been reported in the individuals who have mutations in a conserved 15-bp regulatory hotspot region from the 445T to 449G (Ercu et al., 2020). The mutation in this hotspot region was associated with increased phosphorylation of PDE3A protein, resulting in hypertension with the brachydactyly type E (HTNB) (Maass et al., 2015; van den Born et al., 2016). In the present study, the mutation of tyrosine to cytosine at 497 position may change the status of phosphorylation and protein stability, which may account for decreased activity compared to the wild type.

Changes in enzyme activity caused by changes in amino acid can be due to changes in the active site, conformational structure, protein stability, posttranslational modifications, or increases in sensitivity to protease degradation. The differences observed in enzyme activity may also be caused by different laboratory conditions or human error, which may lead to a misinterpretation of the protein function. In the present study, to avoid intra- and interexperimental variation, we simultaneously transfected a set of variant and wild-type recombinant plasmids (a total of seven including a negative control transfected with vector) with equal amount of the DNA concentration in independent sets of experiments and then studied them to assess the enzyme function. Our data indicated that lower expression of Y497C protein level was observed when compared to the wild-type protein. However, the mRNA expression of the Y497C variant was comparable to that of the wild type. Although the qRT-PCR method may be more accurate, our results from the gene-specific RT-PCR repeatedly showed the same pattern. Therefore, it is presumed that the low protein expression was probably due to the posttranslational modification and this low protein level was expected to have affected the enzyme activity.

The decreased enzyme activity observed was consistent with predictions of in silico analyses of SIFT scores and I-Mutant 3.0 results. All PDE3A missense variants were evaluated with the PolyPhen, SIFT, and I-Mutant 3.0 algorithms to predict protein damage caused by the amino acid mutations (Table 2). The H504Q variant was predicted to be deleterious by the SIFT algorithm, whereas the Y497C, C707R, and A980V variants were only predicted to be damaging by the PolyPhen algorithm. In addition, four of the variants (excluding A980V) were predicted to affect the stability of the protein structure by the I-Mutant 3.0 algorithm.

Since PDE3A is inhibited by cGMP, it cannot be ruled out the possibility that the diminished activity of the PDE3A variant proteins in the present study may be attributed to the increased or altered affinity toward the cGMP.

A number of PDE3A genetic polymorphisms have been identified. Among the mutants discovered, the most studied is the genetic variant associated with HTNB (C. G. Lee et al., 2020). Genetic mutations in the hotspot region of PDE3A gene (exon 4 of PDE3A covering amino acid residues 445–449) has been known to cause an increase in enzyme activity, resulting in the increase in PDE3-Amediated cAMP hydrolysis (Ercu et al., 2020). To date, identified genetic variants from HTNP patients include Thr445Asn, Thr445Ala, Thr445Ser, Thr445del, Ser446Pro, Ala447Thr, Glyaa9Val, and Gly449Asp (C. G. Lee et al., 2020). It is believed that these mutations provide the conformational exposure for additional phosphorylation site for PKA or PKC, which leads to hyperactivation of PDE3A enzyme, resulting in lower cellular cAMP levels (Houslay, 2015). In addition to the missense mutation, a PDE3A promoter polymorphism was identified in heart failure patients, suggesting that altered transcriptional activity by the promoter mutation can cause different responses in the use of PDE3 inhibitors (Sucharov et al., 2019).

Pillai, Staub, and Colicelli (1994) proposed that amino acids 600−722 are important for catalytic activity. The *PDE3A* C707R variant is located in the conserved catalytic region and therefore appears to be evolutionally conserved among the *PDE3* family of genes at the end of the C-terminus. This conserved region may play a key role in maintaining the specific function of PDE3A (Cheung, Yu, Zhang, & Colman, 1998; Pillai et al., 1994). Previous studies have identified a new cAMP-binding amino acid (807Tyr) in the 44 amino acid region that has a flexible loop structure that forms a unique site for the *PDE3* gene family (Hung et al., 2006). A mutagenesis study in the 44 amino acid region showed a 30-fold increase in the K_m value, which suggests that a mutation in this region would play an important role in enzyme activity (Hung et al., 2006). Two missense variants in 44-amino acid region, C707R and A980V, significantly decrease enzyme activity. It was recently demonstrated that thrombin enhances PDE3A enzyme activity in human platelets through a phosphorylation-dependent mechanism that may involve the PI3K/PKB-signaling pathway (Zhang, Ke, Tretiakova, Jameson, & Colman, 2001). The PAR-1 agonist SFLLRN stimulates rapid and transient phosphorylation of PDE3A on the 312Ser, 428Ser, 438Ser, 465Ser, and 492Ser sites. Phosphorylation of these sites on the PDE3A protein has been associated with an increase in PDE3A activity (Hunter, Mackintosh, & Hers, 2009). Missense variants found in the present study could be found close to the phosphorylation sites when the protein is presented as a three-dimensional structure, and this could affect PDE3A activity by disrupting PDE3A phosphorylation.

In summary, we identified 13 *PDE3A* genetic variants and analyzed their frequencies and LD structures. Functional studies of five PDE3A missense variants were performed. All five variants showed a decrease in enzyme activity compared to the wild-type protein. Specifically, the PDE3A Y497C variant showed the most dramatic decrease in cAMP hydroxylation of the test variants. Furthermore, the effects of cilostazol on the *PDE3A* variant proteins resulted in further inhibition of catalytic activity in the PDE3A enzyme. Results from the current study provide useful information that each genetic variant exhibits

a different activity. Further studies are required to determine the relationship between the *PDE3A* variants and the PDE3A mutation-related phenotypes in clinical studies.

Supplementary Material

Refer to Web version on PubMed Central for supplementary material.

ACKNOWLEDGMENTS

This work was supported by a National Research Foundation of Korea (NRF) grant funded by the Korean government (MSIT; No. 2018R1A5A2021242).

Funding information

National Research Foundation of Korea, Grant/Award Number: 2018R1A5A2021242

DATA AVAILABILITY STATEMENT

Data are available on request by contacting the corresponding author Su-Jun Lee.

REFERENCES

Adzhubei IA, Schmidt S, Peshkin L, Ramensky VE, Gerasimova A, Bork P, … Sunyaev SR (2010). A method and server for predicting damaging missense mutations. Nature Methods, 7(4), 248–249. 10.1038/nmeth0410-248 [PubMed: 20354512]

Ahmad F, Murata T, Shimizu K, Degerman E, Maurice D, & Manganiello V. (2015). Cyclic nucleotide phosphodiesterases: Important signaling modulators and therapeutic targets. Oral Diseases, 21(1), e25–50. 10.1111/odi.12275 [PubMed: 25056711]

Ahmad F, Shen W, Vandeput F, Szabo-Fresnais N, Krall J, Degerman E, … Manganiello V. (2015). Regulation of sarcoplasmic reticulum Ca^{2+} ATPase 2 (SERCA2) activity by phosphodiesterase 3A (PDE3A) in human myocardium: Phosphorylation-dependent interaction of PDE3A1 with SERCA2. Journal of Biological Chemistry, 290(11), 6763–6776. 10.1074/jbc.M115.638585 [PubMed: 25593322]

Azevedo MF, Faucz FR, Bimpaki E, Horvath A, Levy I, de Alexandre RB, … Stratakis CA (2014). Clinical and molecular genetics of the phosphodiesterases (PDEs). Endocrine Reviews, 35(2), 195–233. 10.1210/er.2013-1053 [PubMed: 24311737]

Berger M, Raslan Z, Aburima A, Magwenzi S, Wraith KS, Spurgeon BEJ, … Naseem KM (2020). Atherogenic lipid stress induces platelet hyperactivity through CD36-mediated hyposensitivity to prostacyclin: The role of phosphodiesterase 3A. Haematologica, 105(3), 808–819. 10.3324/haematol.2018.213348 [PubMed: 31289200]

Capriotti E, Fariselli P, Rossi I, & Casadio R. (2008). A three-state prediction of single point mutations on protein stability changes. BMC Bioinformatics, 9(Suppl 2), S6. 10.1186/1471-2105-9-S2-S6

Cheung PP, Yu L, Zhang H, & Colman RW (1998). Partial characterization of the active site human platelet cAMP phosphodiesterase, PDE3A, by site-directed mutagenesis. Archives of Biochemistry and Biophysics, 360(1), 99–104. 10.1006/abbi.1998.0915 [PubMed: 9826434]

Choi HI, Kim DY, Choi SJ, Shin CY, Hwang ST, Kim KH, & Kwon O. (2018). The effect of cilostazol, a phosphodiesterase 3 (PDE3) inhibitor, on human hair growth with the dual promoting mechanisms. Journal of Dermatological Science, 91(1), 60–68. 10.1016/j.jdermsci.2018.04.005 [PubMed: 29678305]

Choi YH, Ekholm D, Krall J, Ahmad F, Degerman E, Manganiello VC, & Movsesian MA (2001). Identification of a novel isoform of the cyclic-nucleotide phosphodiesterase PDE3A expressed in vascular smooth-muscle myocytes. Biochemical Journal, 353(Pt 1), 41–50. [PubMed: 11115397]

Chung YW, Lagranha C, Chen Y, Sun J, Tong G, Hockman SC, … Manganiello VC (2015). Targeted disruption of PDE3B, but not PDE3A, protects murine heart from ischemia/reperfusion injury. PNAS, 112(17), E2253–2262. 10.1073/pnas.1416230112 [PubMed: 25877153]

Degerman E, Ahmad F, Chung YW, Guirguis E, Omar B, Stenson L, & Manganiello V. (2011). From PDE3B to the regulation of energy homeostasis. Current Opinion in Pharmacology, 11(6), 676–682. 10.1016/j.coph.2011.09.015 [PubMed: 22001403]

Ercu M, Markó L, Schächterle C, Tsvetkov D, Cui Y, Maghsodi S, … Klussmann E. (2020). Phosphodiesterase 3A and arterial hypertension. Circulation, 142(2), 133–149. 10.1161/circulationaha.119.043061 [PubMed: 32524868]

Francis SH, Busch JL, Corbin JD, & Sibley D. (2010). cGMP-dependent protein kinases and cGMP phosphodiesterases in nitric oxide and cGMP action. Pharmacological Reviews, 62(3), 525–563. 10.1124/pr.110.002907 [PubMed: 20716671]

Heemskerk MM, van den Berg SA, Pronk AC, van Klinken JB, Boon MR, Havekes LM, … van Harmelen, V. (2014). Long-term niacin treatment induces insulin resistance and adrenergic responsiveness in adipocytes by adaptive downregulation of phosphodiesterase 3B. American Journal of Physiology. Endocrinology and Metabolism, 306(7), E808–813. 10.1152/ajpendo.00641.2013 [PubMed: 24473440]

Houslay M. (2015). Hypertension linked to PDE3A activation. Nature Genetics, 47(6), 562–563. 10.1038/ng.3316 [PubMed: 26018892]

Hung SH, Zhang W, Pixley RA, Jameson BA, Huang YC, Colman RF, & Colman RW (2006). New insights from the structure-function analysis of the catalytic region of human platelet phosphodiesterase 3A: A role for the unique 44-amino acid insert. Journal of Biological Chemistry, 281(39), 29236–29244. 10.1074/jbc.M606558200 [PubMed: 16873361]

Hunter RW, Mackintosh C, & Hers I. (2009). Protein kinase C-mediated phosphorylation and activation of PDE3A regulate cAMP levels in human platelets. Journal of Biological Chemistry, 284(18), 12339–12348. 10.1074/jbc.M807536200 [PubMed: 19261611]

Kato N, Loh M, Takeuchi F, Verweij N, Wang X, Zhang W, … Chambers JC (2015). Trans-ancestry genome-wide association study identifies 12 genetic loci influencing blood pressure and implicates a role for DNA methylation. Nature Genetics, 47(11), 1282–1293. 10.1038/ng.3405 [PubMed: 26390057]

Kress AK, Schneider G, Pichler K, Kalmer M, Fleckenstein B, & Grassmann R. (2010). Elevated cyclic AMP levels in T lymphocytes transformed by human T-cell lymphotropic virus type 1. Journal of Virology, 84(17), 8732–8742. 10.1128/JVI.00487-10 [PubMed: 20573814]

Kumar P, Henikoff S, & Ng PC (2009). Predicting the effects of coding non-synonymous variants on protein function using the SIFT algorithm. Nature Protocols, 4(7), 1073–1081. 10.1038/nprot.2009.86 [PubMed: 19561590]

Lee CG, Kang K, Yoon RG, Seo JY, & Park JM (2020). PDE3A variant associated with hypertension and brachydactyly syndrome in a patient with ischemic stroke caused by spontaneous intracranial artery dissection: A review of the clinical and molecular genetic features. European Journal of Medical Genetics, 63(4), 103781. 10.1016/j.ejmg.2019.103781 [PubMed: 31589936]

Lee SJ, Kim WY, Choi JY, Lee SS, & Shin JG (2010). Identification of CYP19A1 single-nucleotide polymorphisms and their haplotype distributions in a Korean population. Journal of Human Genetics, 55(3), 189–193. 10.1038/jhg.2010.6 [PubMed: 20186154]

Maass PG, Aydin A, Luft FC, Schächterle C, Weise A, Stricker S, … Bähring S. (2015). PDE3A mutations cause autosomal dominant hypertension with brachydactyly. Nature Genetics, 47(6),647–653. 10.1038/ng.3302 [PubMed: 25961942]

Movsesian M, Ahmad F, & Hirsch E. (2018). Functions of PDE3 isoforms in cardiac muscle. Journal of Cardiovascular Development and Disease, 5(1), 10. 10.3390/jcdd5010010 [PubMed: 29415428]

Palmer D, & Maurice DH (2000). Dual expression and differential regulation of phosphodiesterase 3A and phosphodiesterase 3B in human vascular smooth muscle: Implications for phosphodiesterase 3 inhibition in human cardiovascular tissues. Molecular Pharmacology, 58(2), 247–252. 10.1124/mol.58.2.247 [PubMed: 10908291]

Pillai R, Staub SF, & Colicelli J. (1994). Mutational mapping of kinetic and pharmacological properties of a human cardiac cAMP phosphodiesterase. Journal of Biological Chemistry,

269(48), 30676–30681. Retrieved from https://www.ncbi.nlm.nih.gov/pubmed/7982987. [PubMed: 7982987]

Reinhardt RR, Chin E, Zhou J, Taira M, Murata T, Manganiello VC, & Bondy CA (1995). Distinctive anatomical patterns of gene expression for cGMP-inhibited cyclic nucleotide phosphodiesterases. Journal of Clinical Investigation, 95(4), 1528–1538. 10.1172/JCI117825 [PubMed: 7706458]

Rondina MT, & Weyrich AS (2012). Targeting phosphodiesterases in anti-platelet therapy. Handbook of Experimental Pharmacology, 210, 225–238. 10.1007/978-3-642-29423-5_9

Rybalkin SD, Yan C, Bornfeldt KE, & Beavo JA (2003). Cyclic GMP phosphodiesterases and regulation of smooth muscle function. Circulation Research, 93(4), 280–291. 10.1161/01.RES.0000087541.15600.2B [PubMed: 12933699]

Sucharov CC, Nakano SJ, Slavov D, Schwisow JA, Rodriguez E, Nunley K, … Bristow MR (2019). A PDE3A promoter polymorphism regulates cAMP-induced transcriptional activity in failing human myocardium. Journal of the American College of Cardiology, 73(10), 1173–1184. 10.1016/j.jacc.2018.12.053 [PubMed: 30871701]

Suzuki Y, Kagawa N, Fujino T, Sumiya T, Andoh T, Ishikawa K, … Tanaka S. (2005). A novel high-throughput (HTP) cloning strategy for site-directed designed chimeragenesis and mutation using the Gateway cloning system. Nucleic Acids Research, 33(12), e109. 10.1093/nar/gni103 [PubMed: 16009811]

Teerlink JR (2009). A novel approach to improve cardiac performance: Cardiac myosin activators. Heart Failure Reviews, 14(4), 289–298. 10.1007/s10741-009-9135-0 [PubMed: 19234787]

Thorlacius EM, Wåhlander H, Ojala T, Ylänen K, Keski-Nisula J, Synnergren M, … Castellheim A. (2020). Levosimendan versus milrinone for inotropic support in pediatric cardiac surgery: Results from a randomized trial. Journal of Cardiothoracic and Vascular Anesthesia, 34(8), 2072–2080. 10.1053/j.jvca.2020.02.027 [PubMed: 32201198]

Traylor M, Amin Al Olama A, Lyytikainen LP, Marini S, Chung J, Malik R, … Markus HS (2020). Influence of genetic variation in PDE3A on endothelial function and stroke. Hypertension, 75(2), 365–371. 10.1161/HYPERTENSIONAHA.119.13513 [PubMed: 31865795]

van den Born BJ, Oskam LC, Zidane M, Schächterle C, Klussmann E, Bähring S, & Luft FC (2016). The case| A handful of hypertension. Kidney International, 90(4), 911–913. 10.1016/j.kint.2016.03.037 [PubMed: 27633875]

Wechsler J, Choi YH, Krall J, Ahmad F, Manganiello VC, & Movsesian MA (2002). Isoforms of cyclic nucleotide phosphodiesterase PDE3A in cardiac myocytes. Journal of Biological Chemistry, 277(41), 38072–38078. 10.1074/jbc.M203647200 [PubMed: 12154085]

Yi M, Cho SA, Min J, Kim DH, Shin JG, & Lee SJ (2017). Functional characterization of a common CYP4F11 genetic variant and identification of functionally defective CYP4F11 variants in erythromycin metabolism and 20-HETE synthesis. Archives of Biochemistry and Biophysics, 620, 43–51. 10.1016/j.abb.2017.03.010 [PubMed: 28347661]

Zewail AM, Nawar M, Vrtovec B, Eastwood C, Kar MN, & Delgado RM 3rd (2003). Intravenous milrinone in treatment of advanced congestive heart failure. Texas Heart Institute Journal, 30(2), 109–113. Retrieved from https://www.ncbi.nlm.nih.gov/pubmed/12809251. [PubMed: 12809251]

Zhang W, Ke H, Tretiakova AP, Jameson B, & Colman RW (2001). Identification of overlapping but distinct cAMP and cGMP interaction sites with cyclic nucleotide phosphodiesterase 3A by site-directed mutagenesis and molecular modeling based on crystalline PDE4B. Protein Science, 10(8), 1481–1489. 10.1110/ps.6601 [PubMed: 11468344]

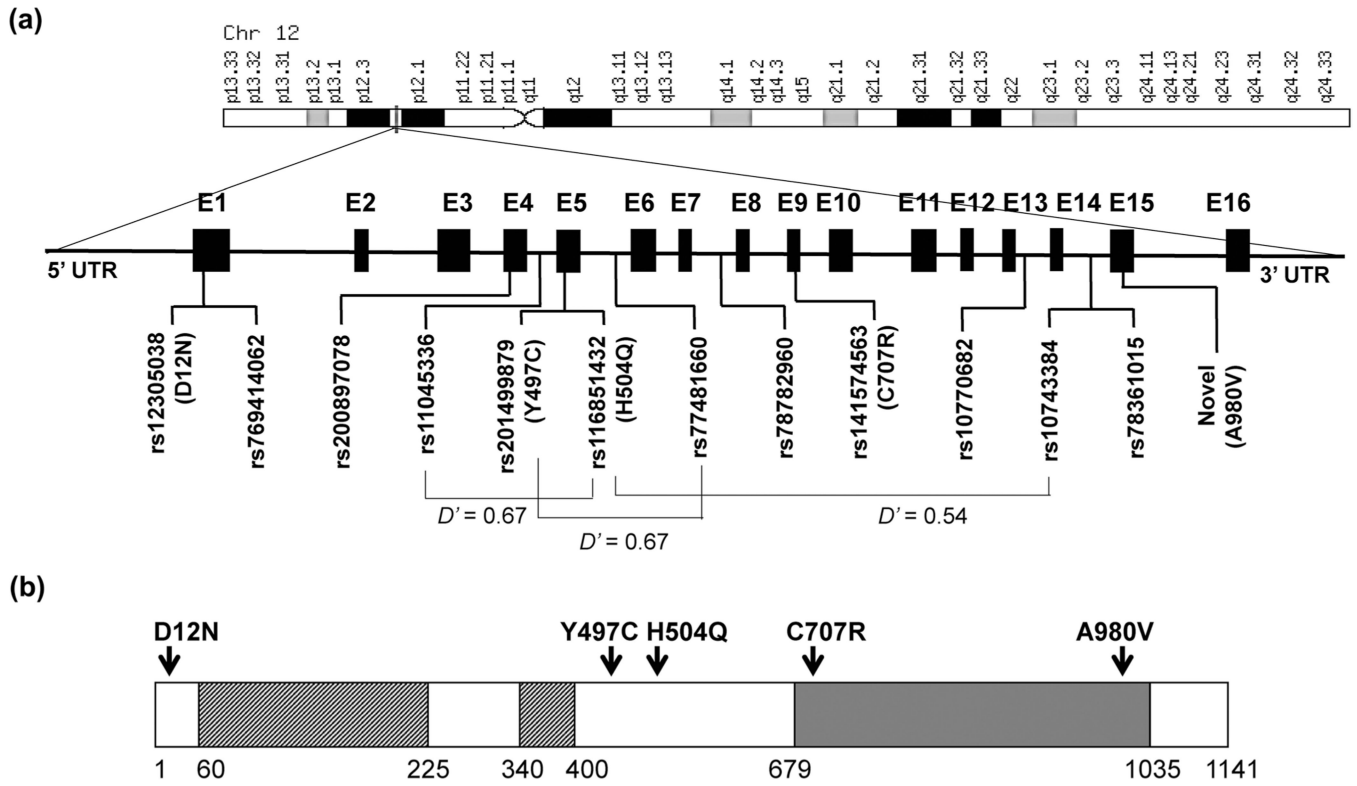

FIGURE 1.

Schematic representation of the *PDE3A* gene structure and LD of *PDE3A* SNPs in the *PDE3A* locus. (a) The *PDE3A* gene consists of 16 exons (black boxes; E1–E16) and 15 introns on chromosome 12. The locations of 13 SNPs are indicated in the map of the *PDE3A* gene. LD analyses between SNP pairs are presented as D values. (b) Functional organization of the PDE3A protein with locations of the identified missense variants. Two N-terminal hydrophobic domains (NHR1 and NHR2) and a C-terminal catalytic domain are indicated on the PDE3A protein structure. Missense variants identified in the present study are indicated by arrows above

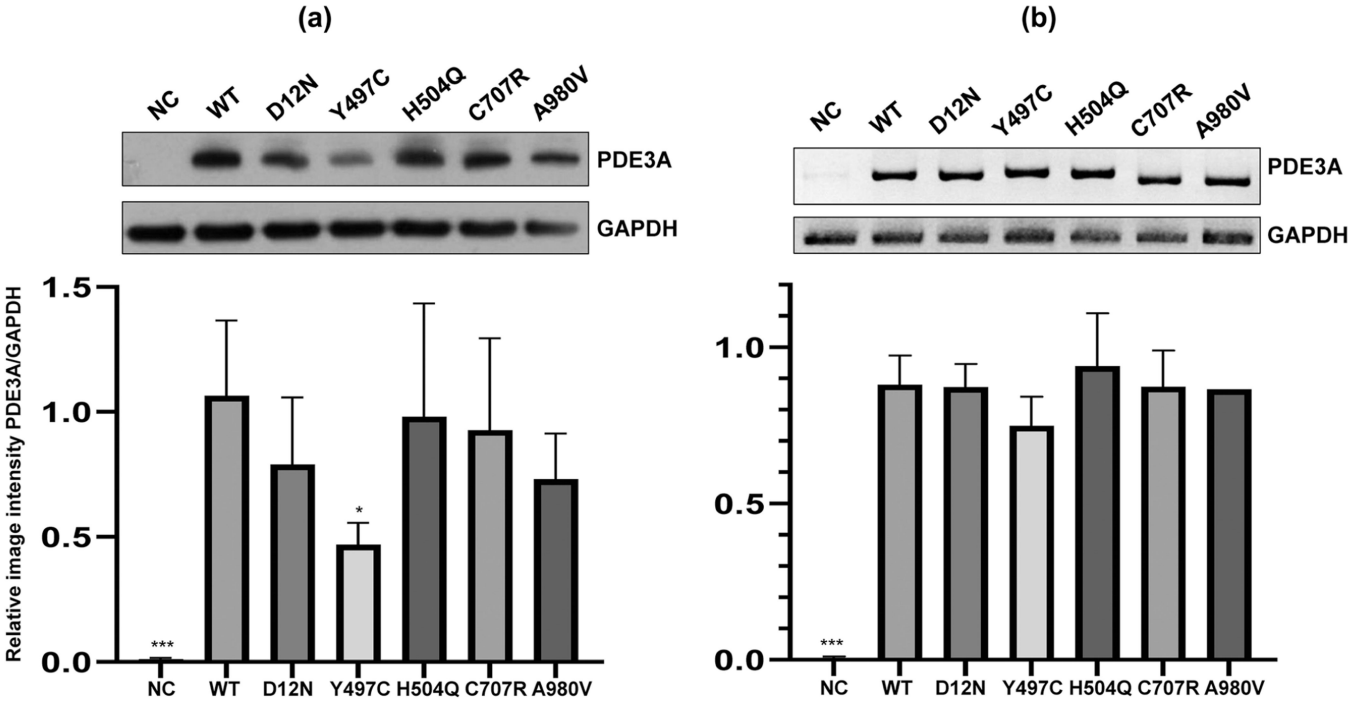

FIGURE 2.

Expression of each PDE3A variant. (a) The expression of each mutant and wild-type protein was examined by Western blotting analyses. Representative results of four independent experiments are shown. All data showed a similar trend. Expression was visualized with Image J. (b) mRNA expression of the *PDE3A* variants. Recombinant plasmids containing *PDE3A* variants were transfected into FreeStyle 293-F cells, and mRNA expression was quantified by gene-specific RT-PCR. Expression was visualized with Image J. Details are described in the Materials and Methods section. All datasets were analyzed by the Shapiro–Wilk test for normality evaluation, and they passed the evaluation. Data were analyzed by one-way ANOVA, and Dunnett's tests for post hoc multiple comparisons. All data are described as means ± SD of each independent value. All experiments were repeated at least three times with triplicates, and representative results are presented. Each p-value was derived from Dunnett's multiple comparison test versus wild type. *$p < .05$,***$p < .001$. NC, negative control; WT, wild type

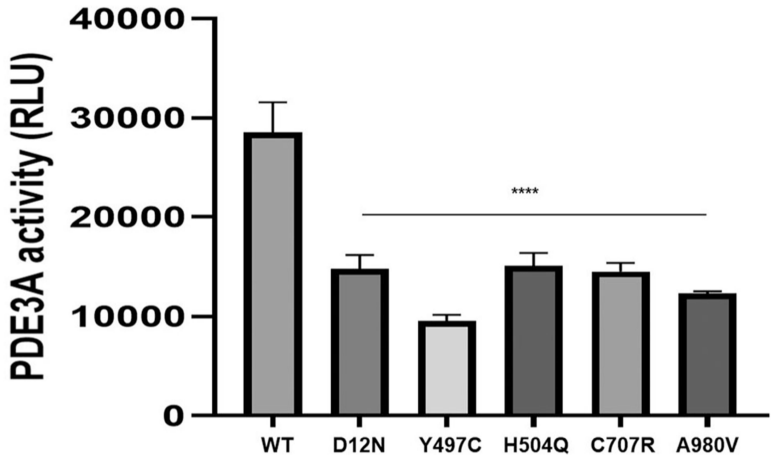

FIGURE 3.

Metabolism of cAMP by wild-type PDE3A protein and recombinant variant proteins. The catalytic activity of PDE3A proteins was determined with a PDE-Glo PDE assay. All variant proteins significantly suppressed PDE activity, accounting for about half of wild-type PDE activity (33–53%). Results are representative of a set of three independent experiments. All datasets were analyzed by the Shapiro–Wilk test for normality evaluation, and they passed the evaluation. Data were analyzed by one-way ANOVA, and Dunnett's tests for post hoc multiple comparisons. All of analyses and graphical visualizations were performed through Prism 8.2.1 (GraphPad Software, San Diego, CA, USA). All data are described as means ± SD of each independent value. All *p*-values of variants' data were lower than .0001, and they were considered as statistically significant. Each *p*-value was derived from Dunnett's multiple comparison test versus wild type. ****$p < .0001$

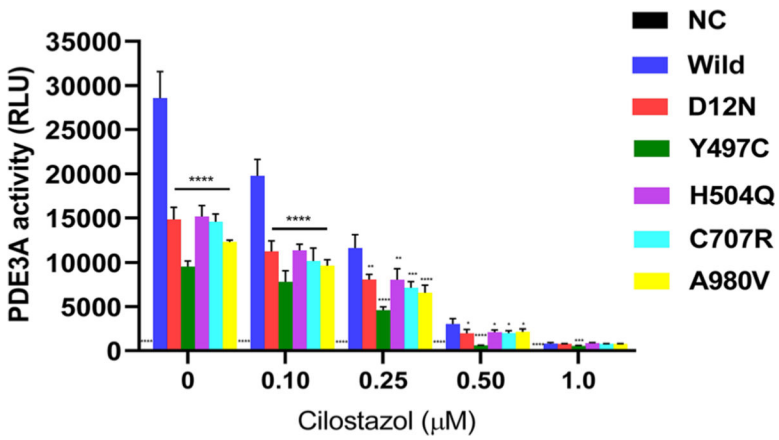

FIGURE 4.

Sensitivity of the PDE3A wild-type and variant proteins to cilostazol. cAMP-specific PDE3A activity was measured in the lysates of transfected FreeStyle 293-F cells with a PDE-Glo assay kit. The PDE3A inhibitor cilostazol was added to the reaction in doses ranging from 0.1 to 1 μM. Details are described in the Materials and Methods section. Values are means ± SD of triplicate assays. All datasets were analyzed by the Shapiro–Wilk test for normality evaluation, and they passed the evaluation. Data were analyzed by one-way ANOVA, and Dunnett's tests for post hoc multiple comparisons. All of analyses and graphical visualizations were performed through Prism 8.2.1 (GraphPad Software, San Diego, CA, USA). All data are described as means ± SD of each independent value. All experiments were repeated at least three times with triplicates, and representative results are presented. Each p-value was derived from Dunnett's multiple comparison test versus wild type. *$p < .05$, **$p < .01$, ***$p < .001$, ****$p < .0001$

TABLE 1

The distribution and comparative analysis of PDE3A SNPs in 50 Koreans

Region	Position	Effect	Reference ID	wt/wt	Wt/Mt	Mt/Mt	Total	MAF (%)	Global (%)	African (%)	European (%)	KRGDB (%)
Exon 1	g.20369318G > A	D12N	rsl2305038	27	18	5	50	28	33.37	50.61	30.91	25.50
Exon 1	g.20369995A > G	R237R	rs769414062	49	1	0	50	1	0.0004	0	0	0.07
Exon 4	g.20616280T > C	T440T	rs200897078	48	2	0	50	2	0.04	0	0	0.72
Intron 4	g.20621151A > G		rsll045336	33	12	5	50	22	12.64	14.30	8.85	23.65
Exon 5	g.20621361A > G	Y497C	rs201499879	48	2	0	50	2	0.06	0	0	1.10
Exon 5	g.20621383T > A	H504Q	rsll6851432	46	4	0	50	4	0.10	0	0	2.40
Intron 5	g.20629808G > C		rs77481660	48	2	0	50	2	0.28	0	0	0.99
Intron 7	g.20633879G > A		rs78782960	48	1	1	50	3	8.13	0.98	10.74	9.45
Exon 9	g.20637217T > C	C707R	rsl41574563	49	1	0	50	1	0.18	0	0	0.96
Intron 13	g.20650332G > A		rsl0770682	40	8	2	50	12	35.32	56.81	34.19	20.75
Intron 14	g.20650615T > C		rsl0743384	5	13	32	50	77	53.97	31.92	63.72	71.67
Intron 14	g.20650634T > C		rs78361015	48	2	0	50	2	0.40	0	0	1.64
Exon 15	g.20653960C > T	A980V	Novel	49	1	0	50	1	na	na	na	na

Each SNP frequency of Global, African, and Europeanwas based on 1000 Genomes, whichwere cited by NCBI dbSNP (https://www.ncbi.nlm.nih.gov/snp). All reference sequences were followed byGRCh38 chromosome 12 and GenBank accession no. NM_000921.5 and NC_000012.12. MAF: minor allele frequency, KRGDB: Database genome browser from the Center for Genome Science of the Korea National Institute of Health (http://coda.nih.go.kr/coda/KRGDB/index.jsp), na: non-available.

TABLE 2

PDE3A function and stability of coding variants as predicted by in silico software

			PolyPhen 2.0		SIFT		I-Mutant 3.0	
Coding variant	**Nucleotide change**[a]	**SNP ID**	**PSIC**	**Prediction**	**Score**	**Prediction**	**DDG**	**Stability**
D12N	C.34G > A	rsl2305038	0.079	Benign	0.31	Tolerated	−1.17	Decrease
Y497C	C.1490A > G	rs201499879	0.89	Damaging	0.21	Tolerated	−2.24	Decrease
H504Q	C.1512T > A C.1512T > C	rsll6851432	0.38	Benign	0.01	Deleterious	−0.42	Decrease
C707R	C.2119T > C	rsl41574563	0.995	Damaging	0.18	Tolerated	−0.54	Decrease
A980V	C.2939C > T	novel	0.992	Damaging	0.05	Tolerated	0.13	Increase

[a]Numbers are given according to the cDNA reference sequence, NM_000921.5.

The function of coding variants was evaluated with the SIFT, PolyPhen 2.0, and I-Mutant 3.0 algorithms. PolyPhen 2.0 calculates position-specific independent count (PSIC) scores for each of two variants. A PSIC score 0.5 or above is considered damaging. SIFT scores ≤ 0.05 are predicted by the algorithm to be intolerant or deleterious amino acid substitutions, whereas scores > 0.05 are considered tolerant. I-Mutant 3.0 computes the predicted free energy change value or sign (DDG), which is calculated from the unfolding Gibbs free energy value of the mutated protein. A positive DDG value indicates that the mutated protein is highly stable.